Mo(VI) dithiocarbamate with no pre-existing Mo–S–Mo core as an active lubricant additive

M. Al Kharboutly, G. Veryasov, P. Gaval, A. Verchere, C. Camp, E.A. Quadrelli, Jules Galipaud, B. Reynard, Manuel Cobian, T. Le Mogne, et al.

Mo(VI) dithiocarbamate with no pre-existing Mo-S-Mo core as an active lubricant additive

M. Al Kharboutly[1], G. Veryasov[2], P. Gaval[2], A. Verchere[2], C. Camp[2], E. A. Quadrelli[2], J. Galipaud[1], B. Reynard[3], M. Cobian[1], T. Le Mogne[1], and C. Minfray[1]

[1] *Université de Lyon, LTDS (UMR5513), Ecole Centrale de Lyon, Ecully, France*

[2] *Université de Lyon, C2P2 (UMR5265), Université de Lyon 1, CPE Lyon, France*

[3] *Université de Lyon, LGL (UMR5276), ENS de Lyon, UCB Lyon1, France*

Abstract (100 words)

MoDTC molecular additives reduce friction in boundary lubricated steel-steel contacts through formation of MoS_2 sheets. The chemical pathway from MoDTC to MoS_2 is investigated for optimizing MoS_2 formation. Our experiments show that a MoDTC molecule containing sulfur only in its thiocarbamate ligands forms MoS_2 sheets during friction, demonstrating that the presence of peripheral thiocarbamate ligands can be sufficient to provide the required sulfur source. This molecule is not only competitive with MoDTC containing sulfur in the core of the molecule but also more efficient at high contact pressures. Mechanistic investigations on the chemical transformation of MoDTC to MoS_2 reveal that thermal activation alone is not sufficient thus suggesting that pressure and/or shear are necessary for MoS_2 generation in this system.

1 Introduction

Energy saving has become a critical societal stake that stimulates drastic technological changes in the transportation and energy sectors [1]. In the field of tribology, reducing friction losses over extended durations is a key challenge. Several solutions have been developed, in particular Transition Metal Dichalcogenides (TMDs), like MoS_2, have been known as efficient solid lubricants for more than fifty years [2–4]. MoS_2 is used in tribological contacts as coating but it can also be formed *in situ* through tribochemical reactions from molecular lubricant additives [5–10]. Among molecular lubricant additives effective under boundary lubrication for steel-steel contacts, the "all-in-one" types of molecules, that is the ones which provide the molybdenum and the sulfur atoms within a single molecule, are commonly used. Molybdenum DiThioCarbamates (MoDTC) are representative examples of these types of molecules (Figure 1).

Even if the mechanism of action of MoDTC has been widely studied, [7–9,11–15] the understanding of the chemical pathway allowing the generation of MoS_2 sheets from the MoDTC molecule is still attracting substantial interest because of the potential insight in novel molecule design. Concerning the elementary steps of MoDTC decomposition, several approaches are found in literature. Initially, only the sulfur atoms present in the core of dimeric molecules, that is as bridging atoms across molybdenum two centers as in (R_2NCS_2) [Mo(O)**(μ-S)$_2$**Mo(O)] (S_2CNR_2) were considered able to contribute to the formation of MoS_2 sheets [8,13]. Later on, it was also proposed that the sulfur atoms from the thiocarbamate ligand, (R_2NC**S$_2$**) [Mo(O)(μ-S)$_2$Mo(O)] (**S$_2$**CNR_2) could be involved in the generation of MoS_2 sheets, either by prior linkage isomerism, as in (R_2NCO**S**) [Mo(***S***)(μ-S)$_2$Mo(O)] (S_2CNR_2) [11,12] or by cleavage of carbon-sulfur bonds of the ligand, schematized as (R_2NC) [(**S$_2$**Mo(O)(μ-S)$_2$Mo(O)**S$_2$**)] (CNR_2) [7,16]. All these approaches suggest that core [Mo_nS_m] fragments called MoS_x intermediate products [7] are needed at some stage in generating well-organized MoS_2 lamellar sheets during friction.

In this work, the performance of a molecular precursor MoDTC **1,** containing only one molybdenum atom and no pre-formed core [Mo_nS_m], is compared with that of a well-established "all-in-one" MoDTC **2** molecule, which contains preformed [Mo(μ-S)$_2$Mo] core classically used in engine lubrication. We show that the tribological properties of molecule MoDTC **1** are competitive with those of well-established MoDTC **2** and show better performances at high contact pressures.

2 Experimental methods

2.1 Lubricant additive synthesis

Two different MoDTC molecules were synthetized (Figure 1). MoDTC **1** has no pre-existing core [Mo-(μ-S)-Mo], nor terminal sulfur atoms (Mo=S) and is in oxidation state Mo(+VI). MoDTC **2** contains the [Mo(μ-S)$_2$Mo] sulphided core and is in oxidation state Mo(+V). Molecule MoDTC **2** is used here as a representative example of the classical molecules used in engine lubrication.

The lubricant composition is prepared in a beaker on a stirrer hot plate by adding a weight percentage of 0.3 w% of each molecule of MoDTC in the synthetic base oil PAO4 at a temperature of 50°C, whilst stirring for 30 min. Solutions were transparent after this mixing procedure showing the good solubility of the additives in base oil.

Note that the atomic concentration of Mo in lubricants containing MoDTC **1** or MoDTC **2** is in the same range since the contribution of Mo to the mass of MoDTC1 (23 wt%) is extremely close to that in MoDTC2 (21 wt%). Thus the difference in molybdenum atomic content in both lubricants is not significant enough to explain potential differences in tribological behaviors. The content of sulfur atoms is a bit larger in MoDTC 1 than in MoDTC 2. As both molecules don't have the same atomic S/Mo ratio (4 for MoDTC **1** and 3 for MoDTC **2**), it is anyway not possible to have the exact same content of molybdenum and sulfur in each lubricant.

• **Synthesis method of MoDTC 1:**

The complex was prepared according to literature [17]. Under air, ammonium molybdate tetrahydrate [$(NH_4)_6Mo_7O_{24}$] • 4 H_2O (3.20 g, 2.59 mmol) was dissolved in 25 mL of distilled water. 3.05 g (13.54 mmol) of sodium diethyldithiocarbamate trihydrate, dissolved in 10 mL of distilled water, were then slowly added over the course of 30 min under vigorous stirring, during which time the colour of the solution gradually turned from yellow to orange and then red with the formation of a precipitate. The red precipitate was isolated on a fritted glass connected to a vacuum Erlenmeyer flask then washed with distilled water (3x10 mL). After washing, the sample was dried under vacuum. Yield, 2.10 g (56 %). Anal. Calcd for $MoC_{10}H_{20}N_2O_2S_4$ (MW= 424.48 g.mol^{-1}): C 28.30, H 4.75, N 6.60; Found C 27.94, H 5.09, N 6.51%.

• **Synthesis method of MoDTC 2:**

The complex was prepared according to the literature [17]. Ammonium molybdate tetrahydrate [$(NH_4)_6Mo_7O_{24}$] • 4 H_2O (4.22 g, 3.41 mmol) was dissolved in 20 mL of distilled water. 30 mL of dimethylformamide (DMF) were poured into the solution and stirred vigorously. Then 9 g of dioctylamine (37.27 mmol) and 30 mL of DMF were added at room temperature. The reaction

medium was cooled in an ice-water bath and finally, 3 mL of carbon disulphide CS_2 (49.65 mmol) were added dropwise over a period of 15 min.

The addition of CS_2 resulted in a gradual colour change of the suspension from white to yellow, then orange and finally purple-red. The solution was then refluxed at 105°C under argon until the colour changed from purple-red to green. The resulting viscous residue was collected on a fritted glass connected to a vacuum Erlenmeyer flask, then washed with acetone (3x50 mL). After washing, a yellow precipitate appeared. After washing, the sample was dried under vacuum Yield, 1.10 g (10 %). Anal. Calcd for $Mo_2C_{34}H_{68}N_2O_2S_6$ (MW = 921.19 $g.mol^{-1}$): C 44.33, H 7.44, N 3.04; Found C 41.13, H 7.10, N 3.78%.

The XPS characterizations of MoDTC **1** and MoDTC **2** are reported in supplementary information (SI 1) and corroborate the structures reported in Figure 1.

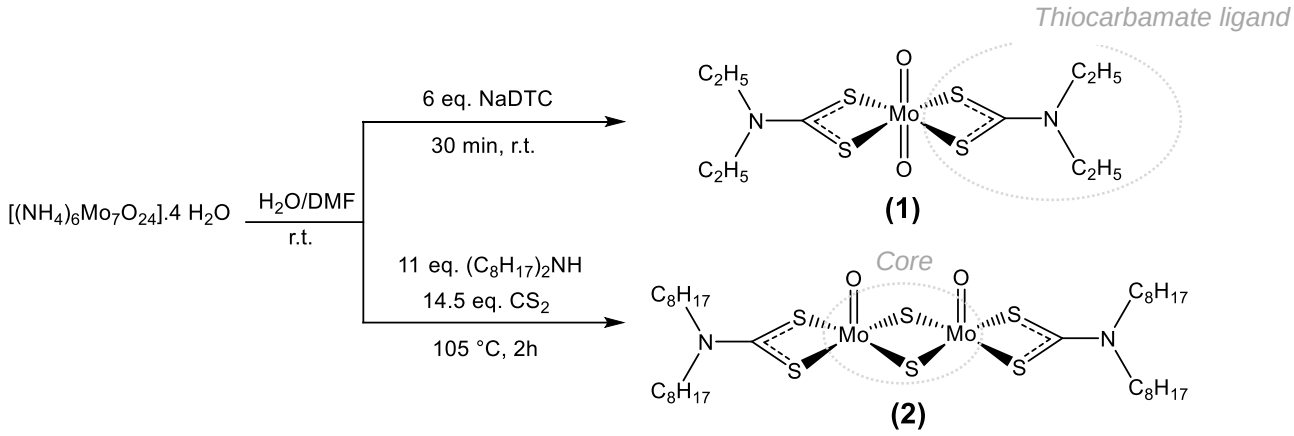

Figure 1: Synthesis of the MoDTC derivatives 1 and 2 (only one linkage isomer represented).

2.2 Friction experiments

Balls and flats counterfaces used for tribotests are both in steel AISI52100. The hardness is around 800 HV. The roughness of the flats and balls are respectively Ra = 12 ± 5 nm and Ra = 40 ± 1 nm. The base oil used is a PAO4. A reciprocating ball-on-flat tribometer [18] was used for tribotests. No external sulfur supply was added to the system. During the test, normal force (strain gage), tangential force (piezoelectric sensor and bi-blades) and temperature (thermocouple type K) were recorded.

Standard conditions of boundary lubrication were as follow: average sliding speed of 56 mm/s, temperature of 100°C and an initial Hertz maximum pressure of 1 GPa (Load of 17 N).

For other tests, the temperature was varied as well as load in order to vary the initial Hertz maximum contact pressure. The contact conditions are summed up in Table1.

Contact conditions	
Samples	Flat ball (R = 6.7 mm)
Load	4 N → 180 N
Speed	56 mm/s
Temperature	20°C, 100°C, 180°C
Stroke length	7 mm
Kinematic	Linear
Frequency	4 Hertz
Maximum Hertz pressure	0.62 GPa → 2.3 GPa
Number of cycles	18000
Immersion volume	80 µL

Table 1: Contact conditions of reciprocating ball-on-flat tribotests.

Representative curves of the friction coefficient as the function of number of cycles are reported. Steady state friction coefficient are calculated from the last 8000 cycles of each test. As tests were repeated at least four times, average steady state friction coefficients and their standard deviations were calculated from the values obtained from the different repeatability tests.

After each test, wear scar diameters were measured by optical microscopy.

2.3 Characterization of tribofilms

All samples were cleaned with *n-heptane* for 10 min in ultrasonic bath before characterization by XPS, Raman spectroscopy and FIB-TEM.

XPS analyses were carried out on a PHI 5000 Versaprobe II apparatus from ULVAC-PHI Inc. A monochromatized AlK_{α} source (1486.6 eV) was used with a spot size of 20 µm. A charge neutralization system is used to limit charge effect. The remaining charge effect was corrected fixing the C-C bond contribution of C1s peak at 284.8 eV. Spectra of $Mo_{3d5/2}$ and S_{2p} regions were obtained using a pass energy of 23.5 eV. All the peaks were fitted with CasaXPS software using a Shirley background. Quantification was carried out using the transmission function of the apparatus and angular distribution correction for a 45° angle. Sensitivity factors were extracted from [19], they integrate cross section and escape depth correction.

Raman spectra were collected using a LabRam HR800 spectrometer from Horiba Scientific. Two different laser wavelengths were used 785 nm (MoDTC **1**) and 532 nm (MoDTC **2** and tribofilms). Typical laser powers of 5 mW were used.

FIB sections were performed across tribofilms for TEM observations. A platinum layer was deposited as a protective layer on tribofilm before nanomachining with Ga^+ ions. Subsequent thinning was carried out to ensure that lamella is thin enough for TEM observations.

The TEM observations were carried out on JEOL2010F equipped with EDS and operating at an accelerating voltage of 200 kV.

Tribofilm compositions could slightly vary in terms of composition regarding position on the wear track. Because of reciprocating oscillatory motion, the contact conditions are most severe at the extremity of wear tracks, where the change of friction directions occurs. The Raman and XPS analyses where done close to these area as the amount of MoS_2 was the most important. Then, some discrepancies in the results between XPS and Raman analyses could be related to the fact that the size of the analyzed area was slightly different for each technics (20 µm of diameter for XPS analyses and around 1 µm for Raman analyses) and to the fact that XPS spectroscopy is more surface sensitive than Raman.

3 Results

3.1 Low friction with MoDTC (1) under standard boundary lubricated conditions

3.1.1 Friction results with MoDTC (1)

MoDTC **1** has been tested under our standard conditions of boundary lubrication (T = 100°C, V = 56 mm/s, $P_{Hertzmax}$ = 1 GPa, 18 000 cycles). The evolution of the friction coefficient as function of the number of cycles is presented in Figure 2.a as well as statistical data processing from several measurements. The average steady state friction coefficient for MoDTC **1** is 0.063 ± 0.001 that is within the range obtained with the reference molecule MoDTC **2** (Figure 2.b - $\mu_{MoDTC\ 2}$ = 0.0644 ± 0.009). The values for the two molecules are statistically similar and in the expected range for the formation of MoS_2 in a boundary lubricated contact [6,15]. It can be also noticed that MoDTC **1** requires longer induction time to reach the low friction steady state regime than MoDTC **2**. No loss of friction reduction capabilities is observed over the full experiment (18000 cycles) for each molecule.

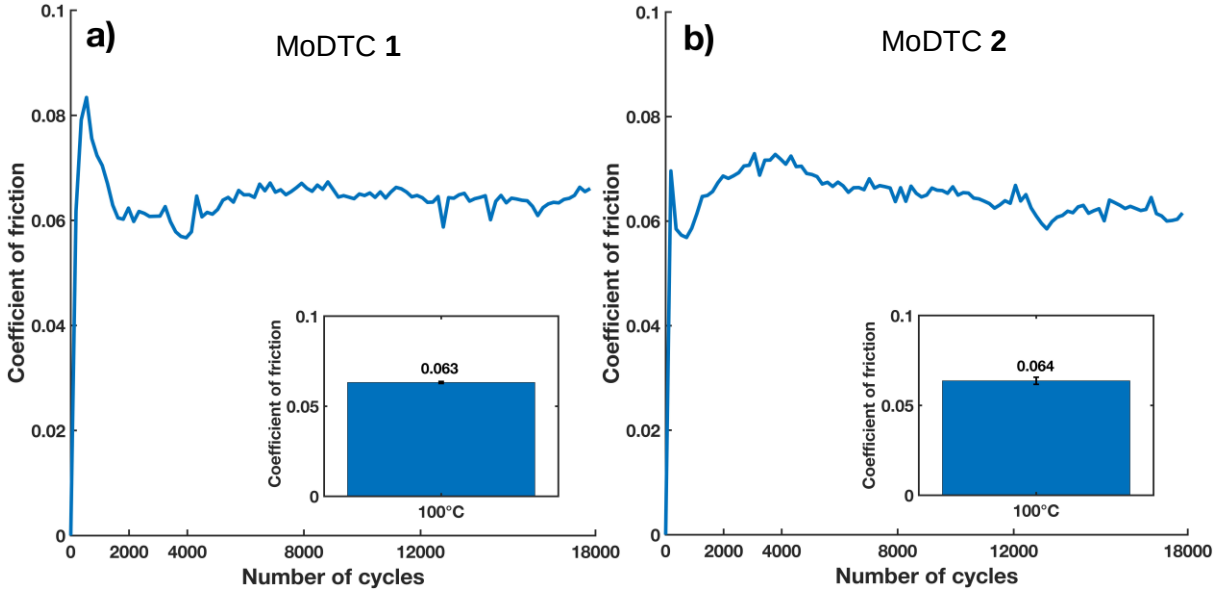

Figure 2: Coefficient of friction at 100°C for a) molecule MoDTC 1 b) molecule MoDTC 2. The tests were performed at an initial maximum Hertz pressure of 1 GPa and an average sliding speed of 56 mm/s. Representative curves of the friction coefficient as the function of number of cycles are shown as well as average steady state friction coefficients calculated from several tests with the related standard deviation.

3.1.2 MoDTC 1 Tribofilm characterization

TEM tribofilm characterizations (Figure 3) confirm the presence of MoS_2 in the tribofilm (flat sample) obtained with MoDTC **1** in the absence of external sulfur supply. In TEM images of tribofilm obtained with MoDTC **1** in standard conditions, MoS_2 sheets are found at the top of the tribofilm of thickness between 30 and 40 nm. The presence of sheets is confirmed by EDS analyses with prominent molybdenum and sulfur peaks, and by interlayer distance around 0.6 nm on HRTEM images, consistent with MoS_2 lamellar sheets observed in tribofilms [15].

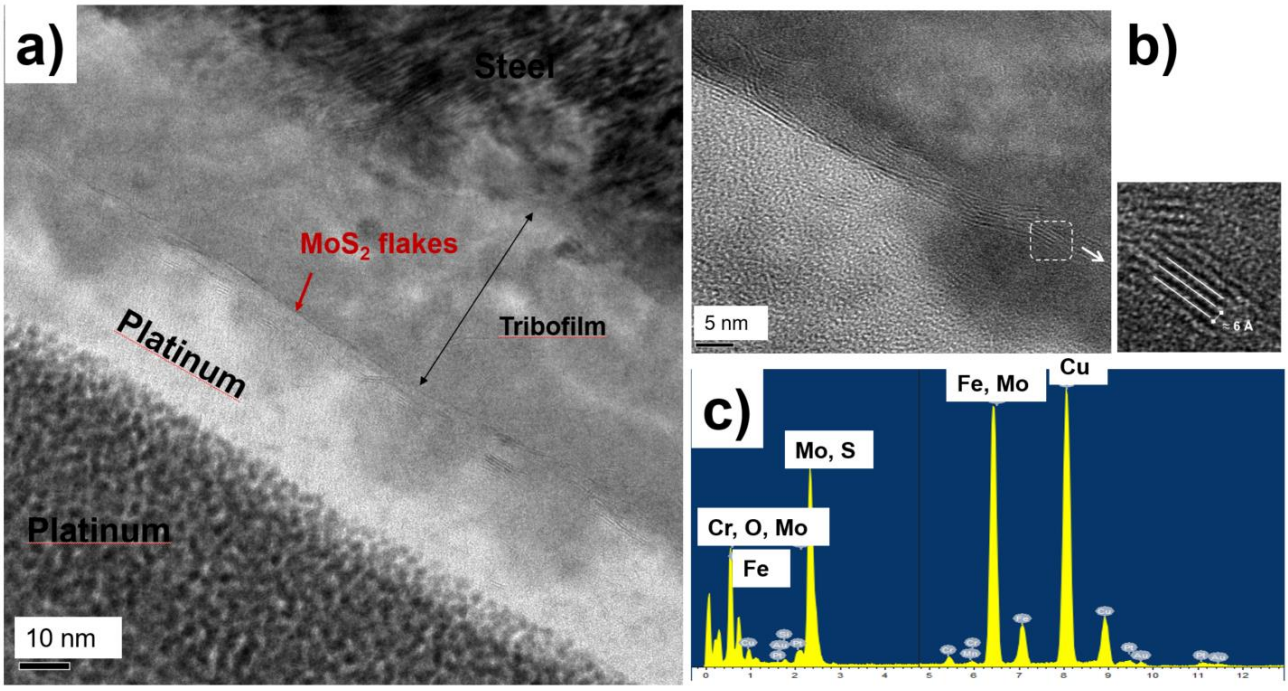

Figure 3: a) and b) TEM images of FIB-cross section of tribofilm (flat) obtained with MoDTC 1 after 18 000 cycles of rubbing under standard contact conditions c) EDX spectrum recorded on the MoS_2 sheets area.

The XPS analysis of the Mo_{3d} and the S_{2p} transitions carried out on the tribofilms obtained after 18 000 cycles with MoDTC **1** at 100°C is reported in Figure 4; details of the fits can be found in Table 2.

Two main molybdenum contributions are found: one with a $Mo_{3d5/2}$ peak around 232.1 eV (Mo_{3d} (C), pink) corresponding to a Mo(+VI) environment related to MoO_3 or $FeMoO_4$ [7,20,21] and another one with a $Mo_{3d5/2}$ peak around 229.0 eV (Mo3d (B), blue) attributed to a Mo(+IV) environment that could correspond to MoS_2 [6,20] or MoS_3 [22,23]. One minor Mo contribution is found at lower binding energy (228.2 eV, Mo_{3d} (A), light blue). This Mo_{3d} (A) contribution at low binding energy is related to a reduced molybdenum species. Such a contribution has been observed on sulfided molybdenum oxide thin films [21,22,24]. It has been proposed to be a defective Mo environment possibly formed in the present context by friction. The peaks near 226 eV (yellow/brown) correspond to sulfur S_{2s} contributions related to S_{2p} contributions discussed in the following paragraph.

The S_{2p} spectrum shows sulfide-type environment at binding energies near 161 eV. The shape and width of the sulfide part of the spectrum leads to the deconvolution of 3 separate contributions. The main S_{2p} (B) contribution at 161.8 eV matches with S^{2-} anion in MoS_2 or in MoS_3. This contribution is consistent with the Mo_{3d} results. A lower binding energy contribution around 161.0 eV S_{2p} (A) would correspond to a more electron-rich sulfur. Such a contribution has been ascribed to sulfur depleted MoS_2 environments that could correspond to the reduced S_{2p} (A) species films [21]. S_{2p} (C) at around 163.1 eV matches either with FeS_2, with thiomolybdate or $(S_2)^{2-}$ in MoS_3 [22].

To summarize, XPS analyses performed at 100°C after tribotest under standard conditions in presence of MoDTC **1** suggest that MoS_2 is the main Mo based compound present at the top surface of the tribofilm. This is supported by quantification of sulfur (S_{2p} (A) and (B)) over molybdenum (Mo (B)) species characteristic of MoS_2 yielding a S/Mo ratio close to 2. MoS_3 could be also considered as peak position of Mo_{3d} (B), S_{2p} (B) and S_{2p} (C) are in agreement with [22], but in much lower amount compared to MoS_2 regarding the at% of S_{2p}(C) peak (Figure 4 and Table 2).

Sample Id.	Element/Transition	Peak energy (eV)	FWHM (eV)	Atomic concentration (at %)	Assignment
MoDTC 1	***$Mo_{3d5/2-3/2}$***				
	Mo_{3d} - (A)	228.2 - 231.4	1.2	6.1	Reduced MoS_2
	Mo_{3d} - (B)	229.0 - 232.2	1.7	25.3	MoS_2 ou MoS_3
	Mo_{3d} - (C)	232.1 - 235.3	1.7	11.9	MoO_3 / $FeMoO_4$
	$S_{2p3/2-1/2}$				
	S_{2p} - (A)	161 - 162.1	1.1	13.6	S^{2-} in reduced MoS_2
	S_{2p} - (B)	161.8 - 162.9	1.1	37.7	S^{2-} in MoS_2 or in MoS_3
	S_{2p} - (C)	163.1 - 164.2	1.1	5.4	$(S_2)^{2-}$ in FeS_2 or thiomolybdate or MoS_3

Table 2: Peak fitting details related to Figure 4 e.i. XPS analyses of tribofilms obtained with MoDTC 1 after 18 000 cycles of rubbing at 100°C at an initial maximum Hertz pressure of 1 GPa and an average sliding speed of 56 mm/s.

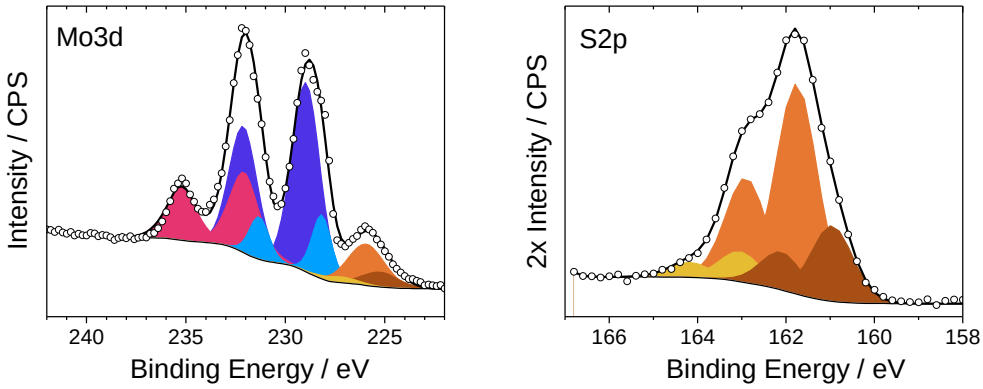

Figure 4: XPS analyses (Mo3d) carried out of tribofilms (flats) obtained with MoDTC 1 after 18 000 cycles of rubbing at 100°C at an initial maximum Hertz pressure of 1 GPa and an average sliding speed of 56 mm/s.

The characteristic Raman analyses of the tribofilm obtained at 100°C under standard conditions with MoDTC **1** are presented in Figure 5. The two MoS_2 characteristic Raman shifts E^1_{2g} and A_{1g} at 373 cm^{-1} and 405 cm^{-1}, respectively, are detected, in agreement with Raman analyses of MoDTC tribofilms [10,14,25]. The presence of amorphous MoS_3 compound [26] could explain the background shape near E^1_{2g} and A_{1g}. The presence of $Fe(MoO_4)$ is suggested by the presence of the Raman peak at 925 cm^{-1} [7] and is consistent with the Mo (+VI) oxide contribution detected by XPS at 232.3 eV on Mo_{3d} peak.

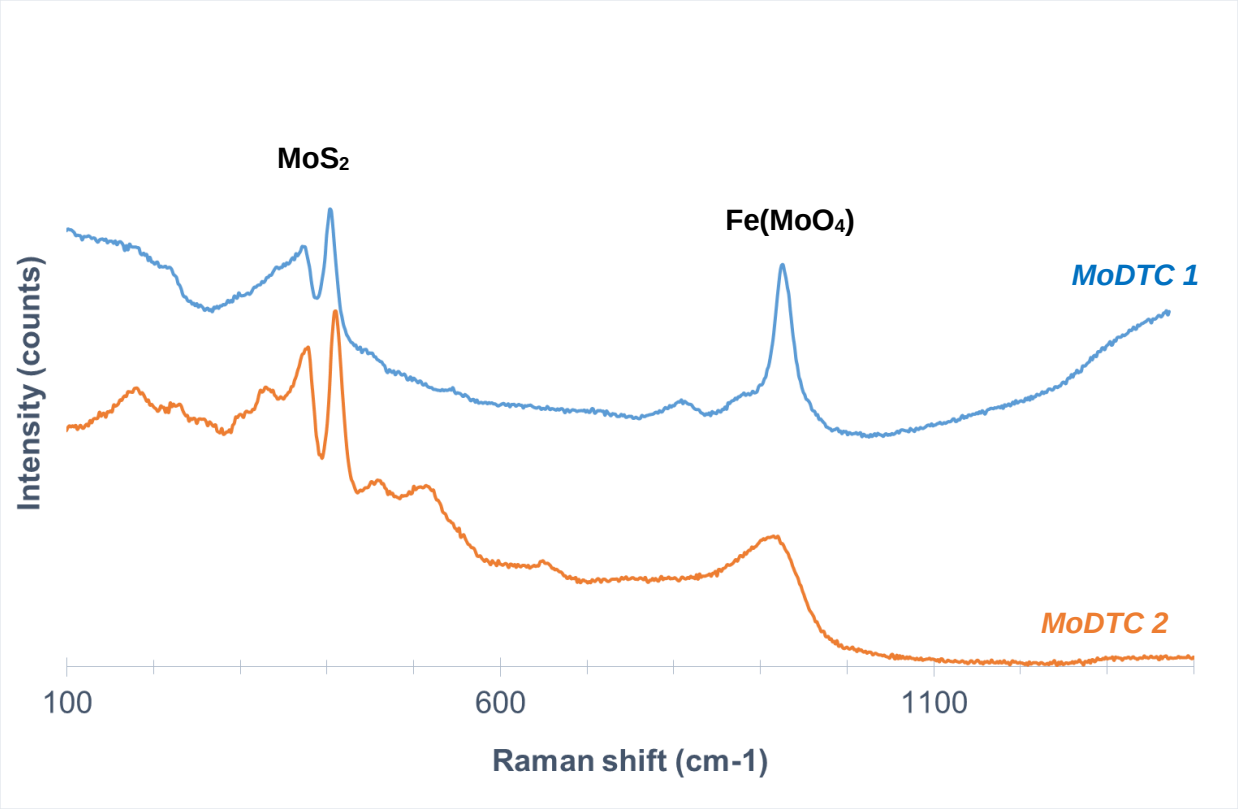

Figure 5: Raman analyses on tribofilms (flats) obtained with MoDTC 1 and MoDTC 2 after 18 000 cycles of rubbing at 100°C at an initial maximum Hertz pressure of 1 GPa and an average sliding speed of 56 mm/s.

3.1.3 MoDTC 2 Tribofilm characterization

Raman (Figure 5) and XPS (Figure 6 and Table 3) characterizations were also performed on tribofilm obtained with MoDTC **2** at 100°C and 1 GPa for comparison with MoDTC **1**. Both results show the presence of MoS_2 and $FeMoO_4$ for MoDTC **2** tribofilm, like for MoDTC **1**. This is in accordance with literature works since XPS analyses of tribofilm obtained with MoDTC often propose the presence of two main contributions attributed to Mo+IV and Mo+VI [15,27]. The presence of molybdenum oxysulfide (purple contribution B' in Figure 6 and table 3) is also detected for MoDTC **2** tribofilm by XPS and was previously suggested in literature [6,20].

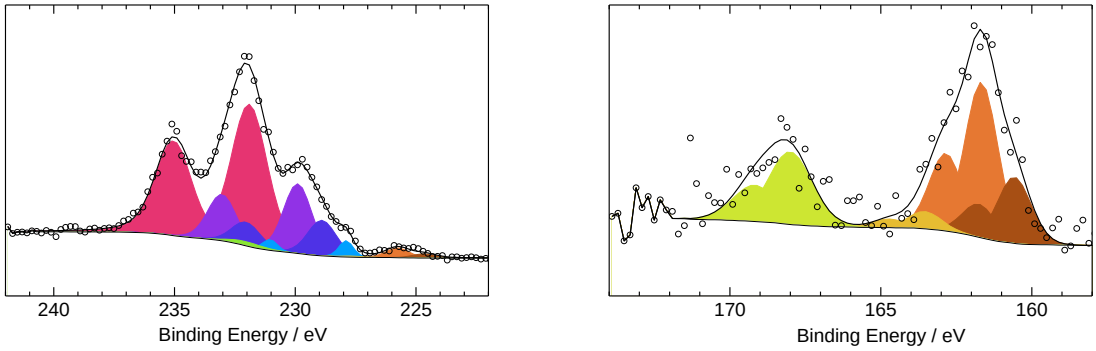

Figure 6: XPS analyses (Mo3d) carried out of tribofilms (flats) obtained with MoDTC 2 after 18 000 cycles of rubbing at 100°C at an initial maximum Hertz pressure of 1 GPa and an average sliding speed of 56 mm/s.

Sample Id.	Element/Transition	Peak energy (eV)	FWHM (eV)	Atomic concentration (at%)	S (at%) /Mo (at%) ratio)	Assignement
MoDTC 2	***$Mo_{3d5/2-3/2}$***				0.5	
	Mo_{3d} - (A)	227.9- 231.0	0.7	1.7		Reduced MoS_2
	Mo_{3d} - (B)	228.9 - 232.0	1.4	7.4		MoS_2 or MoS_3
	Mo_{3d} - (B')	229.9- 233.0	1.4	14.6		MoO_xS_y
	Mo_{3d} - (C)	231.9 – 235.0	1.8	42.0		MoO_3 / $FeMoO_4$
	$S_{2p3/2-1/2}$					
	S_{2p} - (A)	160.6 – 161.8	1.3	6.7		S^{2-} in reduced MoS_2
	S_{2p} - (B)	161.7 - 162.9	1.3	15.8		S^{2-} in MoS_2 or in MoS_3
	S_{2p} - (C)	163.6 - 164.9	1.3	1.9		$(S_2)^{2-}$ in FeS_2, thiomolybdate MoO_xS_y or MoS_3
	S_{2p} - (E)	168.0 – 169.2	1.3	10		Sulfate

Table 3: Peak fitting details related to Figure 6 e.i. XPS analyses of tribofilms obtained with MoDTC 2 after 18 000 cycles of rubbing at 100°C at an initial maximum Hertz pressure of 1 GPa and an average sliding speed of 56 mm/s.

3.2 Effect of temperature

3.2.1 Friction and wear results

The friction performances of molecules MoDTC **1** and MoDTC **2** have been studied at three different temperatures (T = 20°C, 100°C and 180°C at V = 56 mm/s, $P_{Hertzmax}$ = 1 GPa, Figure 7).

The optimal tested temperature for both molecules is 100°C as a durable and low friction regime is achieved in both cases (cf §3.1.1).

At 20°C, MoDTC **2** performs only marginally worse than at 100°C, while MoDTC **1** significantly underperforms (μ = 0.074 vs 0.099, respectively). Considering the overall monotonous decrease of the friction coefficients over the whole experiment (Total number of cycles = 18 000) for both molecular lubricants, it might be possible that neither system has reached steady state by the end of the experiment. Given the more pronounced decrease of the friction coefficient (both in terms of starting absolute value and in terms of overall drop) for MoDTC **1** than for MoDTC **2**, the induction process seems more pronounced for MoDTC **1** than for MoDTC **2**.

At 180°C, the loss of friction reduction capabilities is observed after a few thousand cycles for both MoDTC **1** and MoDTC **2** and very high friction coefficient are observed for most of the experiment, leading to high (apparent) steady state coefficients.

The wear behaviors obtained with the two molecules over the three temperatures appear to follow the same trend as the apparent steady state coefficients described above (cf Figure 8). The lowest wear is found at 100°C for both molecules MoDTC **1** and MoDTC **2**, with MoDTC **1** still marginally outperforming MoDTC **2** (width of the wear = 180 μm vs. 222 μm, respectively). Both wear (MoDTC **1** and MoDTC **2** at 100°C) are just slightly superior to Hertz diameter (red line) which represent the size of the contact before friction without any wear. The loss in performance at 20°C is more noticeable for MoDTC **1** than for MoDTC **2** (width of the wear = 558 μm vs. 299 μm, respectively). The poorest performances are observed at 180°C for both lubricants (width of the wear = 620 μm for MoDTC **1** and 650 μm for MoDTC **2**).

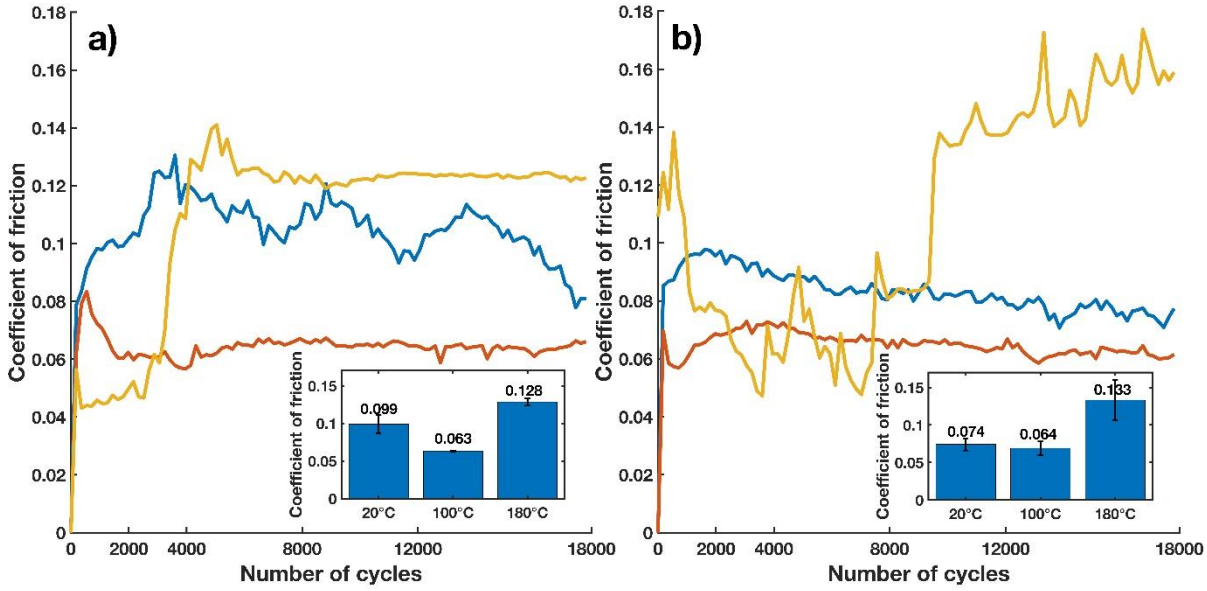

Figure 7: Coefficient of friction at 20°C (blue), 100°C (orange) and 180°C (yellow) for a) molecule MoDTC 1 b) molecule MoDTC 2. The tests were performed at an initial maximum Hertz pressure of 1 GPa and an average sliding speed of 56 mm/s. Representative curves of the friction coefficient as the function of number of cycles are shown as well as average steady state friction coefficients calculated from several tests with the related standard deviation.

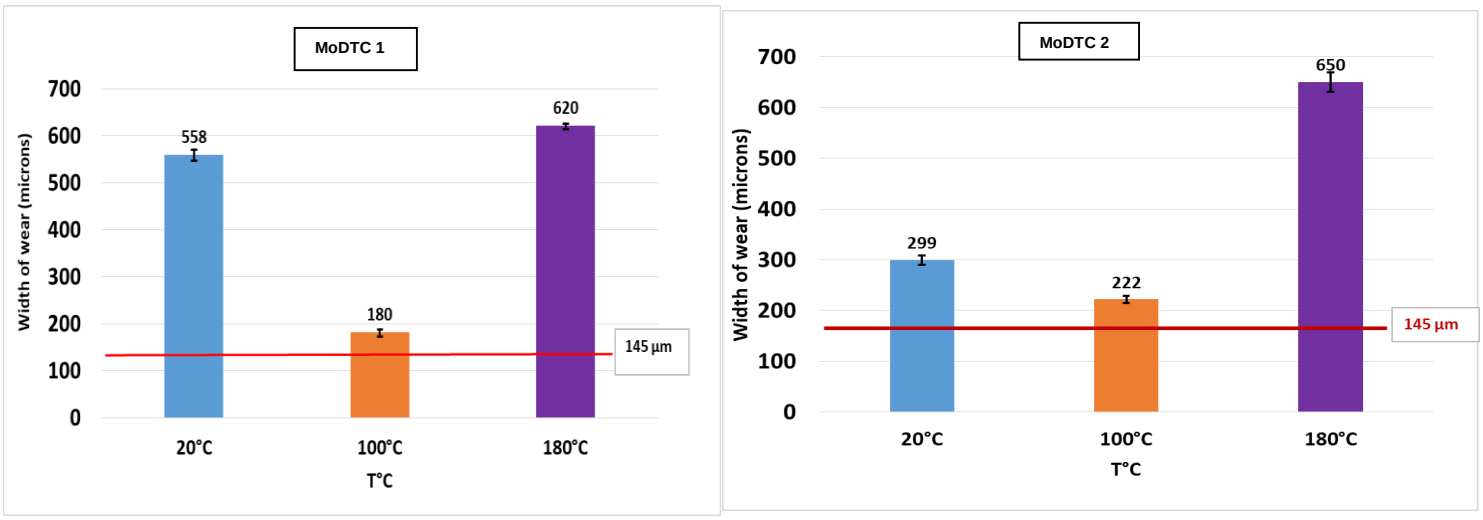

Figure 8: Width of ball wear obtained at 20°C, 100°C and 180°C for a) molecule MoDTC 1 b) molecule MoDTC 2. The tests were performed at an initial maximum Hertz pressure of 1 GPa and an average sliding speed of 56 mm/s. The red line represents the Hertz diameter (size of the contact before friction).

3.2.2 Tribofilm characterizations with MoDTC 1 at 20°C, 100°C and 180°C (XPS and Raman)

The XPS analyses of the Mo_{3d} and the S_{2p} transitions carried out on the tribofilms obtained with MoDTC **1** at different temperatures after 18 000 cycles are reported in Figure 9; details of the fits can be found in Table 4.

The fit explanation of the tribofilm obtained at 100°C is detailed in § 3.1.2.

For the tribofilm at 20°C, only one Mo environment is found around 232.1 eV (Mo_{3d} (C), pink) corresponding to a Mo(+VI) environment related to MoO_3 or $FeMoO_4$. Significant amount of SO_x species is found but no evidence of MoS_2 is detected.

For the tribofilm at 180°C, two Mo environments are found. The main one with a $Mo_{3d5/2}$ peak around 232.1 eV (Mo_{3d} (C), pink) corresponds to a Mo(+VI) environment related to MoO_3 or $FeMoO_4$. The Mo_{3d} (B') contribution (229.9 eV, purple) at binding energy higher than MoS_2 but lower than a typical Mo(+VI) signal could correspond to oxysulfide species MoO_xS_y [6,20]. SO_x species are also detected.

385

Sample Id.	Element/Transition	Peak energy (eV)	FWHM (eV)	Atomic concentration (at%)	Assignment
MoDTC 1 20°C	***$Mo_{3d5/2-3/2}$***				
	Mo_{3d} - (C)	232.2 - 235.4	1.3	54.0	MoO_3 / $FeMoO_4$
	$S_{2p3/2-1/2}$				
	S_{2p} - (B)	162.1 - 163.2	1.7	8.3	$(S_2)^{2-}$ in FeS_2 or Fe thiomolybdate
	S_{2p} - (D)	166.4 - 167.5	1.5	12.4	SO_3 species
	S_{2p} - (E)	168.3 - 169.4	1.5	25.3	Sulfate
MoDTC 1 100°C	***$Mo_{3d5/2-3/2}$***				
	Mo_{3d} - (A)	228.2 - 231.4	1.2	6.1	Reduced MoS_2
	Mo_{3d} - (B)	229.0 - 232.2	1.7	25.3	MoS_2 ou MoS_3
	Mo_{3d} - (C)	232.1 - 235.3	1.7	11.9	MoO_3 / $FeMoO_4$
	$S_{2p3/2-1/2}$				
	S_{2p} - (A)	161 - 162.1	1.1	13.6	S^{2-} in reduced MoS_2
	S_{2p} - (B)	161.8 - 162.9	1.1	37.7	S^{2-} in MoS_2 or in MoS_3
	S_{2p} - (C)	163.1 - 164.2	1.1	5.4	$(S_2)^{2-}$ in FeS_2 or thiomolybdate or MoS_3
MoDTC 1 180°C	***$Mo_{3d5/2-3/2}$***				
	Mo_{3d} - (B')	229.9 - 233.0	1.9	26.2	MoO_xS_y
	Mo_{3d} - (C)	232.0 - 235.1	1.3	46.2	MoO_3 / $FeMoO_4$
	$S_{2p3/2-1/2}$				
	S_{2p} - (B)	163.0 - 164.1	1.7	9.0	$(S_2)^{2-}$ in FeS_2 or thiomolybdate
	S_{2p} - (E)	168.3 - 169.4	1.7	18.6	Sulfate

386

387 ***Table 4: Peak fitting details related to Figure 9 e.i. XPS analyses of tribofilms obtained***
388 ***with MoDTC 1 after 18 000 cycles of rubbing at 20°C, 100°C and 180°C at an initial***
389 ***maximum Hertz pressure of 1 GPa and an average sliding speed of 56 mm/s***

390

391

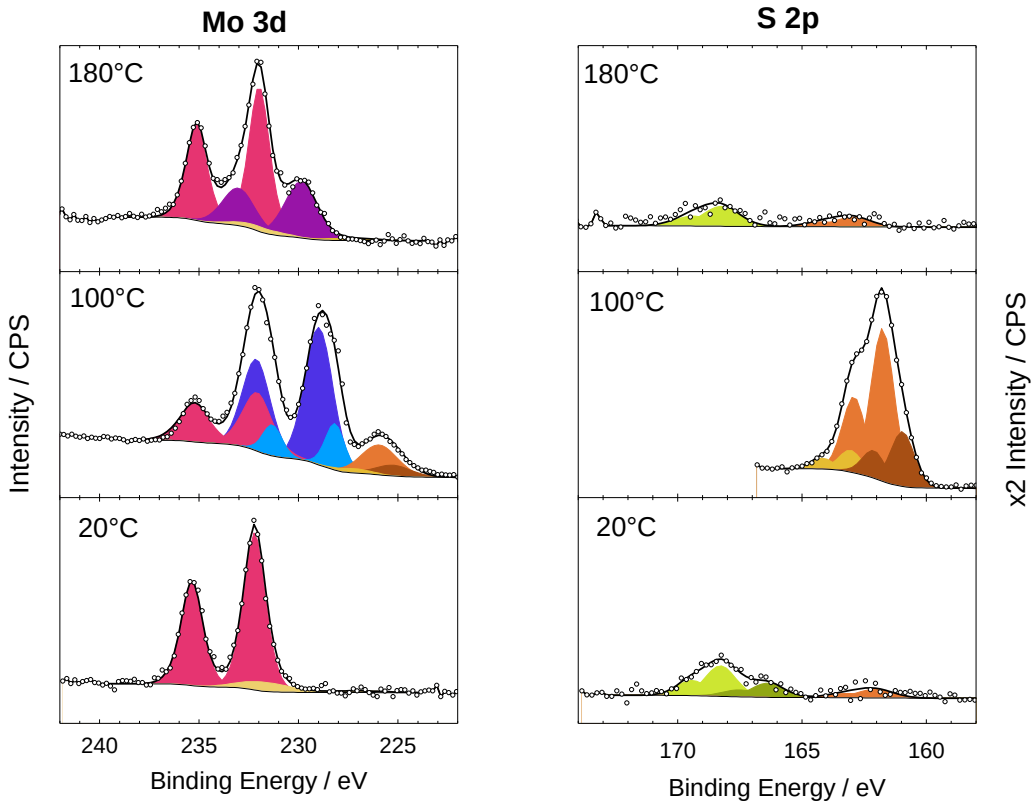

Figure 9: XPS analyses (Mo3d) carried out of tribofilms (flats) obtained with MoDTC 1 after 18 000 cycles of rubbing at 20°C. 100°C and 180°C at an initial maximum Hertz pressure of 1 GPa and an average sliding speed of 56 mm/s (see text for further details).

The Raman analyses of the MoDTC **1** tribofilms obtained at 20°C, 100°C and 180°C are presented in Figure 10.

At 20°C, the observed peaks are mostly related to iron oxides (Fe_2O_3 and Fe_3O_4), like at 180°C [28] and molybdenum based species like MoO_3 are poorly detected [29]. Atomic ratio Mo/Fe calculated from XPS data ($Mo/Fe_{20°C}$ = 0.5 - $Mo/Fe_{100°C}$ = 2.9 - $Mo/Fe_{180°C}$ = 0.9) suggests that the amount of molybdenum compared to iron in tribofilms is much smaller at 20°C and 180°C than at 100°C. As Raman technic is much less surface sensitive than XPS, it could explain why such molybdenum-based compounds are poorly detected by Raman technics at 20°C and 180°C.

At 100°C, the two MoS_2 characteristic peaks E^1_{2g} and A_{2g} at 373 cm^{-1} and 405 cm^{-1}, respectively are detected. The presence of amorphous MoS_3 compound could explain the background shape near E^1_{2g} and A_{2g}. The presence of Fe(MoO_4) at 100°C is suggested by the presence of the Raman peak at 925 cm^{-1} and is consistent with the Mo (+VI) oxide contribution detected by XPS at 232.3 eV on Mo3d peak.

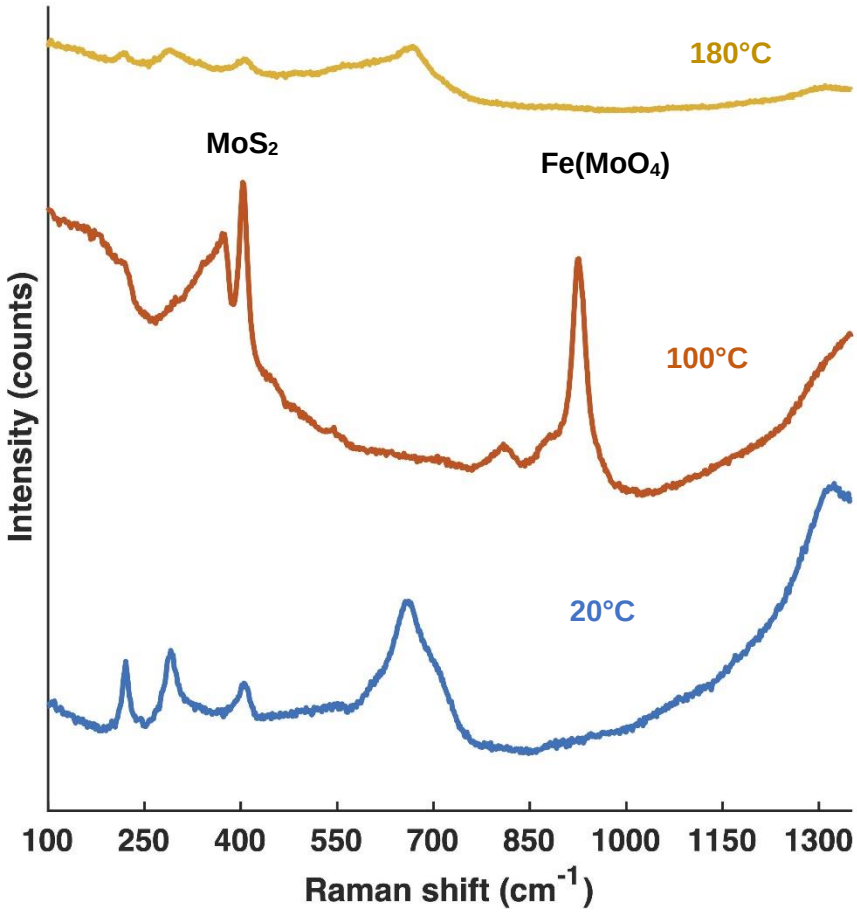

Figure 10: Raman analyses on tribofilms (flats) obtained with MoDTC 1 after 18 000 cycles of rubbing at 20°C. 100°C and 180°C at an initial maximum Hertz pressure of 1 GPa and an average sliding speed of 56 mm/s.

3.2.3 Tribofilm characterizations with MoDTC **2**

XPS and Raman analyses of tribofilms obtained with MoDTC **2** at 20°C are reported in Figures SI 2-1 and SI 2-2 for comparison. Like for tribofilm obtained with MoDTC **1** at 20°C, Mo+VI contribution is mostly detected by XPS on Mo3d peak as well as sulfate on S2p peak. The composition of the tribofilm dominated by molybdenum oxide at temperatures around 20°C-30°C was already observed in literature for such type of MoDTC [15,27].

The comparison of tribofilm composition of MoDTC **1** and MoDTC **2** at 100°C was presented in §3.1.3. As found in literature [15,27], the Mo+IV contribution (MoS_2) increases in tribofilms obtained at higher temperatures, up to 80°C-100°C. Rai *et al.* [14] and Komaba *et al.* [15] have also suggested that such temperatures have an effect on the structural organization of the MoS_2 layers.

For temperatures higher than 100°C, only few data are found in literature [27].

3.3 Effect of contact pressure

3.3.1 Friction results

Friction results obtained at 100°C for the two molecules MoDTC **1** and MoTDC **2** at different initial maximum Hertz pressures (from 0.6 to 2.3 GPa) are reported in Figure 11 (V = 56 mm/s. T = 100°C, 18 000 cycles). Average steady state friction coefficients obtained from repeated tests and observed standard deviations are reported.

At low contact pressures, the friction behavior at the steady state is similar for the two molecules within standard deviations. Above an initial maximum Hertz contact pressure of 1.9 GPa, significant differences in friction behavior appear between the two molecules: MoDTC **1** still achieves a low friction regime whereas MoDTC **2** does not.

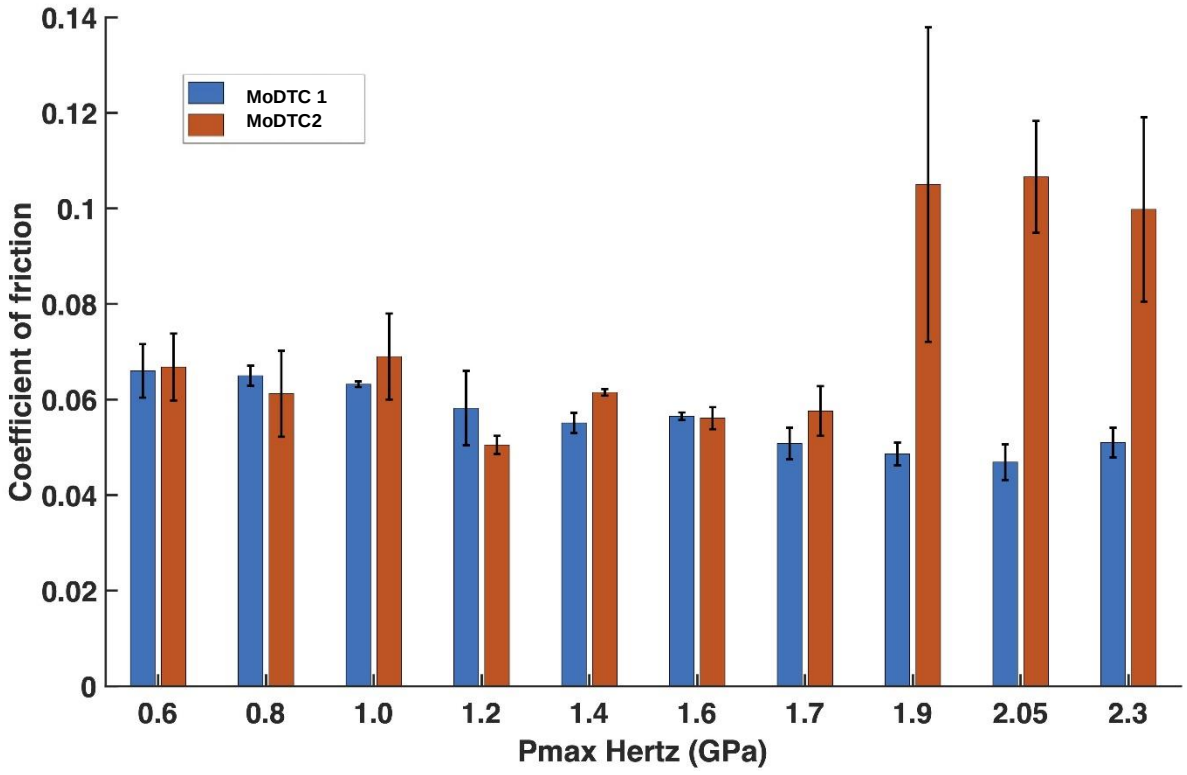

Figure 11: Average steady state friction coefficient for different Initial Hertz maximum contact pressures for molecule MoDTC 1 and molecule MoDTC 2. The tests were performed at a temperature of 100°C and an average sliding speed of 56 mm/s. Average steady state friction coefficients are calculated from several tests with the related standard deviation.

3.3.2 Tribofilms characterization

The XPS and Raman characterizations performed on tribofilms obtained with MoDTC **1** at different contact pressures are shown respectively in Figure 12/Table 5 and Figure 13.

The interpretation of the XPS data follows the results presented in §3.1.2. For all tested contact pressures, beside the main contributions (Mo_{3d} (B), blue) attributed to MoS_2 or MoS_3, Mo (+VI) oxide contributions attributed to $Fe(MoO_4)$ is also found in significant amount (namely, Mo_{3d} (C), pink and 925 cm^{-1} Raman peak). At high contact pressures, Mo_{3d} (B) is the main contribution, and Mo_{3d} (C) dominates at low contact pressure (0.8 GPa). The low binding energy Mo_{3d} (A) contribution is detected mainly at low contact pressures (0.8 GPa and 1 GPa) and would correspond to defective MoS_2. No oxysulfide-type molybdenum is evidenced (binding energies expected between Mo3d (B) and Mo3d (C)) [6,20,22].

Concerning the S_{2p} spectra, two main characteristic sulfur environments are found with no clear dependence on contact pressure: a sulfide-type environment at low binding energies ($S_{2p3/2}$ < 164 eV) and a SO_x type environment at higher binding energies ($S_{2p3/2}$ > 166 eV) characteristic of oxidized sulfur.

In Raman spectra, different components, MoS_2, $Fe(MoO_4)$, amorphous MoS_3 and carbonaceous matrix [30] are identified. It is difficult to further interpret the observed differences as they may be related to the localization of the analyzed area within the heterogeneous wear track, rather than to systematic dependence on contact pressure.

499

Sample Id.	Element/Transition	Peak energy (eV)	FWHM (eV)	Atomic concentration (at%)	S (at%) /Mo (at%) ratio)	Assignement
MoDTC 1 0.8 GPa	***$Mo_{3d5/2-3/2}$***				1.6	
	Mo_{3d} - (A)	227.9 - 231.1	1.4	3.7		Reduced MoS_2
	Mo_{3d} - (B)	228.7 - 231.9	2.0	6.7		MoS_2 or MoS_3
	Mo_{3d} - (C)	231.8 - 235.0	2.0	28.2		MoO_3 / $FeMoO_4$
	$S_{2p3/2-1/2}$					
	S_{2p} - (A)	161.0 - 162.1	1.0	25.6		S^{2-} in reduced MoS_2
	S_{2p} - (B)	162.1 - 163.3	1.0	11.9		S^{2-} in MoS_2 or in MoS_3
	S_{2p} - (C)	163.0 - 164.1	1.0	10.8		$(S_2)^{2-}$ in FeS_2 or thiomolybdate or MoS_3
	S_{2p} - (E)	168.6 - 169.8	1.7	13.1		Sulfate
MoDTC 1 1 GPa	***$Mo_{3d5/2-3/2}$***				1.3	
	Mo_{3d} - (A)	228.2 - 231.4	1.2	6.1		Reduced MoS_2
	Mo_{3d} - (B)	229.0 - 232.2	1.7	25.3		MoS_2 or MoS_3
	Mo_{3d} - (C)	232.1 - 235.3	1.7	11.9		MoO_3 / $FeMoO_4$
	$S_{2p3/2-1/2}$					
	S_{2p} - (A)	161 - 162.1	1.1	13.6		S^{2-} in reduced MoS_2
	S_{2p} - (B)	161.8 - 162.9	1.1	37.7		S^{2-} in MoS_2 or in MoS_3
	S_2p - (C)	163.1 - 164.2	1.1	5.4		$(S_2)^{2-}$ in FeS_2 or thiomolybdate or MoS_3
MoDTC 1 1.4 GPa	***$Mo_{3d5/2-3/2}$***				2.3	
	Mo_{3d} - (B)	229.0 - 231.1	1.4	21.2		MoS_2 or MoS_3
	Mo_{3d} - (C)	232.4 - 235.6	1.6	9.1		MoO_3 / $FeMoO_4$
	$S_{2p3/2-1/2}$					
	S_{2p} - (A)	160.8 - 161.9	1.1	5.3		S^{2-} in reduced MoS_2
	S_{2p} - (B)	161.7 - 162.9	1.1	33.0		S^{2-} in MoS_2 or in MoS_3
	S_{2p} - (C)	163.3 - 164.4	1.1	4.6		$(S_2)^{2-}$ in FeS_2 or thiomolybdate or MoS_3
	S_{2p} - (D)	166.7 - 167.9	1.6	11.7		SO_3 species
	S_{2p} - (E)	168.8 - 170.0	1.6	15.1		Sulfate
MoDTC 1 2 GPa	***$Mo_{3d5/2-3/2}$***				1.55	
	Mo_{3d} - (B)	228.8 - 231.9	1.6	26.5		MoS_2 or MoS_3
	Mo_{3d} - (C)	231.9 - 235.1	2.0	12.6		MoO_3 / $FeMoO_4$
	$S_{2p3/2-1/2}$					
	S_{2p} - (A)	160.5 - 161.7	1.1	13.6		S^{2-} in reduced MoS_2
	S_{2p} - (B)	161.5 - 162.7	1.1	38.8		S^{2-} in MoS_2 or in MoS_3
	S_{2p} - (C)	162.6 - 163.8	1.1	8.5		$(S_2)^{2-}$ in FeS_2 or thiomolybdate or MoS_3

500

501 ***Table 5: Peak fitting details related to Figure 12 e.i. XPS analyses of tribofilms obtained***
502 ***with MoDTC 1 after 18 000 cycles of rubbing at 100°C at an initial maximum Hertz***
503 ***pressure of 0.8 GPa, 1 GPa, 1.4 GPa, 2 GPa and an average sliding speed of 56 mm/s***

504

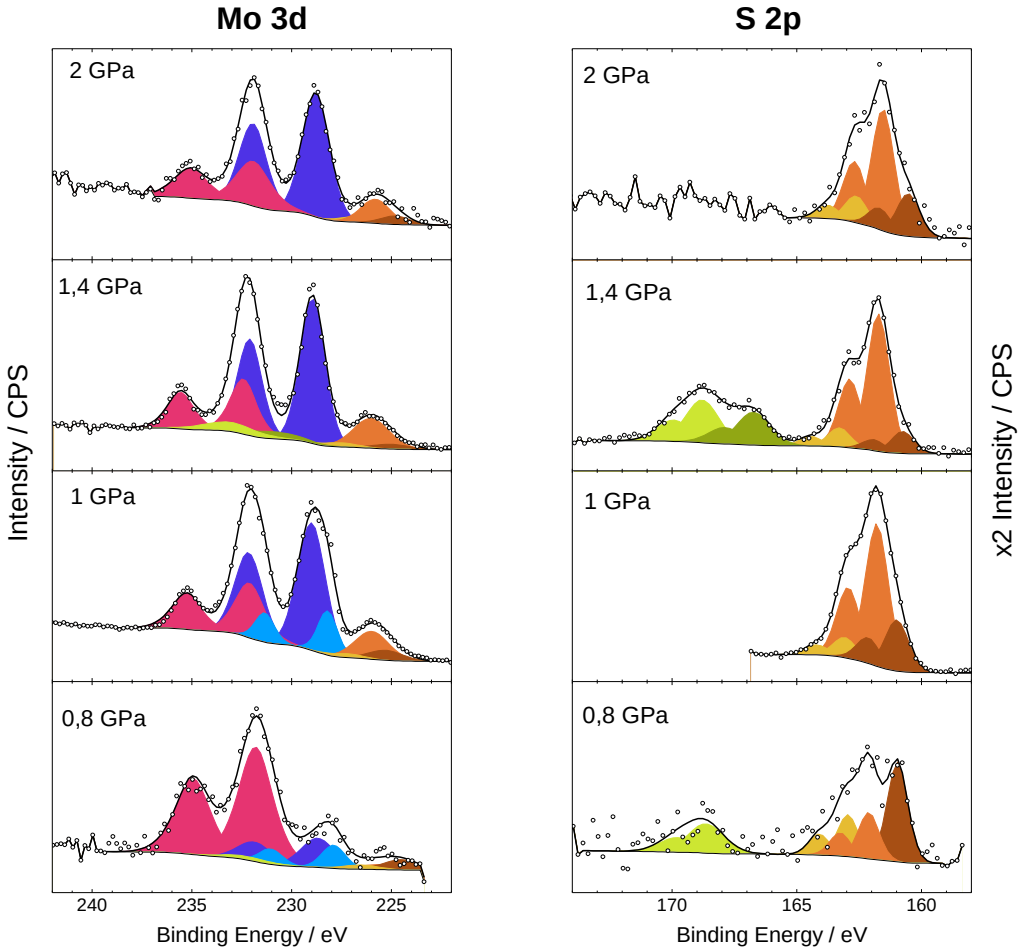

Figure 12: XPS analyses (Mo3d peak) carried out of tribofilms (flats) obtained with MoDTC 1 at various initial maximum Hertz pressure after 18 000 cycles of rubbing at 100°C and an average sliding speed of 56 mm/s.

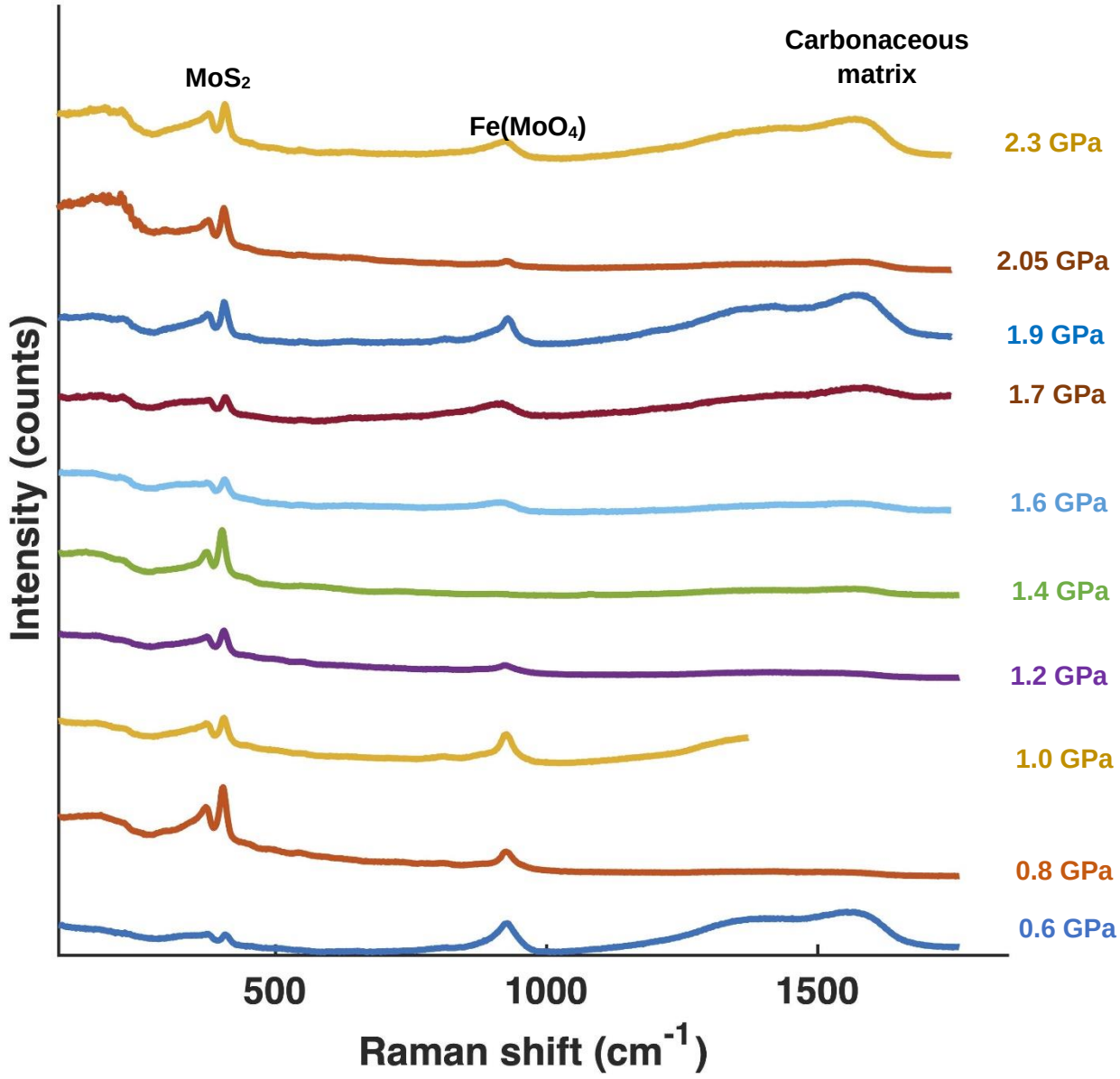

Figure 13: Raman analyses on tribofilms (flats) obtained with MoDTC 1 after 18 000 cycles of rubbing at different initial maximum Hertz pressure, at 100°C and at an average sliding speed of 56 mm/s.

XPS and Raman analyses of tribofilms obtained with MoDTC **2** at 0.8 GPa and 1.2 GPa are reported in Figures SI 2-3, SI 2-4 and SI 2-5 for comparison with MoDTC **1**. Like for tribofilms obtained with MoDTC **1,** MoS_2 is mainly detected by Raman and XPS. The low binding energy Mo_{3d} (A) contribution detected by XPS and that would correspond to defective MoS_2 analyses is also mainly detected at low contact pressures (0.8 GPa) like for MoDTC 1.The peak at 925 cm^{-1} on Raman spectra attributed to $Fe(MoO_4)$ seems more significant in case of MoDTC **1** than for MoDTC **2**.

3.4 Effect of temperature without contact pressure and shear

To test if the decomposition of both MoDTC molecules toward MoS_2 can be thermally induced (with no other concurrent reagent), we performed Raman analyses after thermal degradation for both molecules at different temperatures in air and under argon atmosphere (Figure 14) in the absence of steel material. At high temperature (160°C for open air tests and 120°C for argon atmosphere tests), the molecule MoDTC **1** is decomposed but no MoS_2 formation is observed. In contrast, Raman spectra obtained from 260°C both in air and Ar atmosphere with MoDTC **2** exhibits Raman peaks around 400 cm^{-1}. This is not compatible with MoO_3 and MoO_2 [31] but that could be related to Mo-S vibrations. The E^1_{2g} and A_{1g} peaks are found at slightly lower positions than standard MoS_2 analyzed at ambient temperature, but this may be due the temperature dependence of the peak position with temperature [32] or to the fact that it is more a MoS_x compound rather than MoS_2 [33]. The decomposition in MoS_2 of MoDTC closed to MoDTC **2** structure by thermal degradation was already found in literature [34].

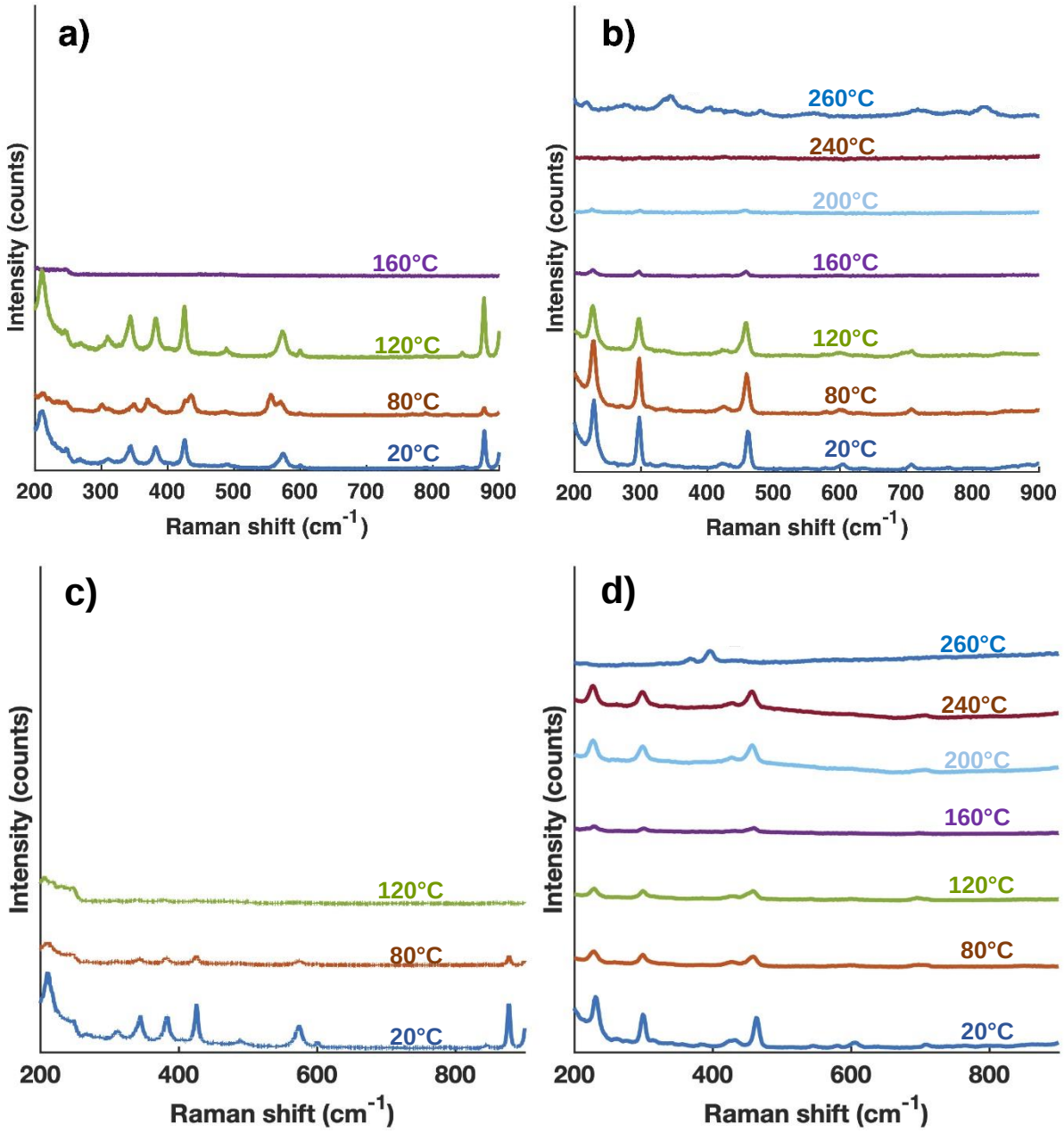

Figure 14: Raman analyses performed on pure additives in different atmosphere and at different temperatures: a) MoDTC 1 in air (laser wavelength 784 nm) and b) MoDTC 2 in air (laser wavelength 532 nm) c) MoDTC 1 under argon atmosphere (laser wavelength 784 nm) and d) MoDTC 2 under argon atmosphere (laser wavelength 532 nm).

4 Discussion

The achievement of low friction coefficients (0.05 to 0.07) under boundary lubrication in steel-steel contact was observed for both molecules MoDTC **1** and MoDTC **2**, and is concurrent with the formation of MoS_2. The originalities of MoDTC **1** are to outperform MoDTC **2** at high contact pressures, and to allow MoS_2 formation without a preformed dimeric core in the molecule, external sulfur supply, and with a high starting oxidation number (Mo(+VI)). Such distinctive chemical properties open mechanistic questions on how such MoDTC molecules can lead to the formation of MoS_2.

Concerning the oxidation state of molybdenum atom within the molecule, systems with a Mo(+VI) molybdate core have been described but they need to be blended with other additives to form MoS_2 sheets [26]. Among the potential reductive sources, the organic oil or the organic ligands could play a chemical reducing role, but the formation of iron-molybdate involving both iron coming from the steel surface and molybdenum from the additive supports the idea of an active role of steel in these phenomena. This is further corroborated by the fact that MoS_2 is not observed upon thermal heating of MoDTC powder in the absence of steel (results §3.4) and by the fact that molybdate is the main detected phase under less severe conditions at low contact pressure (Figures 12 and 13). Therefore, it can be suggested that the steel-steel contact lubricated with oil environment is reducing enough to reduce Mo(+VI) in MoDTC **1** into Mo(+IV), in the absence of other additives.

The two MoDTC molecules display a very different response during thermal degradation. Additive MoDTC **2** seems to degrade into MoS_x compounds in both air and argon atmospheres near 260°C. This is in agreement with reported mechanism on thermal degradation of such molecules containing the $[Mo(\mu\text{-}S)_2Mo]$ sulphided core as MoDTC **2** [34]. Conversely, as shown on Figures 14, MoS_2 is not formed from MoDTC **1** during thermal degradation. This suggests a strong role of mechanical stresses and a chemical role of iron. Consistently, we have evidenced the formation of MoS_2 from MoDTC **1** only in wear tracks of tribotests (Figures 3 and 4). As shown above, mechanical stresses for MoDTC **2** action does not seem necessary for forming MoS_2, as it seems to form in thermal degradation experiments, but they may positively add to thermal degradation and/or chemical role of steel surface.

To summarize, MoDTC **1** is an interesting molecular additive to reduce friction in boundary lubricated steel-steel contacts. This efficient molecule achieves high performance up to high contact pressures by accessing mechanistic pathways that could be distinct from those of classical molecules such as MoDTC **2** or molybdate [26]**.** We ruled out the formation of MoS_2 by a mechanism based solely on the thermal degradation of MoDTC **1**. The absence of core

sulfur in molecule MoDTC **1** also rules out (at least in the initial stages) the chemical degradation mechanism proposed by Grossiord *et al.* [8] where only sulfur atoms present in the core of the molecule contribute to the MoS_2 generation. The necessary involvement of the sulfur atoms in the ligands of MoDTC **1** remains compatible with at least two proposed mechanisms: the formation of a Linkage Isomer - MoDTC [11,12], or the cleavage of carbon-sulfur bonds of the ligand [7,16]. Then, MoS_x intermediate products seems needed before generating well-organized MoS_2 lamellar sheets during friction as it was proposed previously [7,26].

5 Conclusion

In this work, the tribological properties and factors influencing the formation of MoS_2 from {$[MoO_2](S_2CNEt_2)_2$} (MoDTC **1**) and {$[Mo_2(S/O)_4](S_2CNOc_2)_2$} (MoDTC **2**) were investigated. Unexpectedly, MoDTC **1**, comprising Mo(+VI) and containing sulfur atoms only in its thiocarbamate ligands, is able to form MoS_2 sheets in lubricated steel/steel contacts under boundary lubrication conditions. This experimental study therefore demonstrates that, contrary to what was classically assumed, the presence of peripheral thiocarbamate ligands can be sufficient to provide the required sulfur source in these “all-in-one” types of molecules. This molecule is not only competitive with “classical” MoDTC used in engine lubrication, containing sulfur in the core of the molecule, but is even more powerful at high contact pressures.

On the mechanistic point of view, this work confirms that the chemical pathway from MoDTC to MoS_2 is not only thermal. Pressure and shear take an important role in the tribochemical reactions route leading to the formation of MoS_2. A substantial contribution of the surface, as mentioned in the discussion section, remains an important parameter to consider as well.

Those results give insights in molecule design and lubricant formulation to improve MoS_2 sheets generation from several types of contact conditions

6 Acknowledgments

The authors thank “Institut Carnot I@L” for financial support (Projet MoST AAP2016). The FIB cross section have been done at Manutech-USD in Saint-Etienne (France). Electron Beam Microscopy have been done at the “Centre des technologies et des microstructures”, Claude Bernard University of Lyon (France). The Raman facility at LGL-TPE ENS de Lyon is also supported by INSU-CNRS and by the LABEX Lyon Institute of Origins (ANR-10-LABX-0066) of the Université de Lyon within the program "Investissements d'Avenir" (ANR-11-IDEX-0007) of the French government operated by the National Research Agency (ANR).

BIBLIOGRAPHY

[1] Holmberg K, Erdemir A. The impact of tribology on energy use and CO_2 emission globally and in combustion engine and electric cars. Tribol Int 2019;135:389–96. https://doi.org/10.1016/j.triboint.2019.03.024.

[2] Singer IL, Bolster RN, Wegand J, Fayeulle S, Stupp BC. Hertzian stress contribution to low friction behavior of thin MoS2 coatings. Appl Phys Lett 1990;57:995–7. https://doi.org/10.1063/1.104276.

[3] Donnet C, Martin JM, Le Mogne T, Belin M. Super-low friction of MoS_2 coatings in various environments. Tribol Int 1996;29:123–8. https://doi.org/10.1016/0301-679X(95)00094-K.

[4] Fleischauer PD, Lince JR. Comparison of oxidation and oxygen substitution in MoS_2 solid film lubricants. Tribol Int 1999;32:627–36. https://doi.org/10.1016/S0301-679X(99)00088-2.

[5] Spikes H. Friction Modifier Additives. Tribol Lett 2015;60. https://doi.org/10.1007/s11249-015-0589-z.

[6] De Feo M, Minfray C, De Barros Bouchet MI, Thiebaut B, Le Mogne T, Vacher B, et al. Ageing impact on tribological properties of MoDTC-containing base oil. Tribol Int 2015;92:126–35. https://doi.org/10.1016/j.triboint.2015.04.014.

[7] Khaemba DN, Neville A, Morina A. New insights on the decomposition mechanism of Molybdenum DialkyldiThioCarbamate (MoDTC): a Raman spectroscopic study. RSC Adv 2016;6:38637–46. https://doi.org/10.1039/C6RA00652C.

[8] Grossiord C, Varlot K, Martin J-M, Le M, Esnouf C, Inoue K. MoS_2 single sheet lubrication by molybdenum dithiocarbamate. Tribol Int 1998;31:737–43. https://doi.org/10.1016/S0301-679X(98)00094-2.

[9] Komaba M, Kondo S, Suzuki A, Kurihara K, Mori S. Kinetic study on lubricity of MoDTC as a friction modifier. Tribol Online 2019;14:220–5. https://doi.org/10.2474/trol.14.220.

[10] Okubo H, Yonehara M, Sasaki S. In Situ Raman Observations of the Formation of MoDTC-Derived Tribofilms at Steel/Steel Contact Under Boundary Lubrication. Tribol Trans 2018;61:1040–7. https://doi.org/10.1080/10402004.2018.1462421.

[11] Deshpande P, Minfray C, Dassenoy F, Mogne TL, Jose D, Cobian M, et al. Tribocatalytic behaviour of a TiO_2 atmospheric plasma spray (APS) coating in the presence of the friction modifier MoDTC: a parametric study. RSC Adv 2018;8:15056–68. https://doi.org/10.1039/C8RA00234G.

[12] Onodera T, Miura R, Suzuki A, Tsuboi H, Hatakeyama N, Endou A, et al. Development of a quantum chemical molecular dynamics tribochemical simulator and its application to tribochemical reaction dynamics of lubricant additives. Model Simul Mater Sci Eng 2010;18:034009. https://doi.org/10.1088/0965-0393/18/3/034009.

[13] Peeters S, Restuccia P, Loehlé S, Thiebaut B, Righi MC. Characterization of Molybdenum Dithiocarbamates by First-Principles Calculations. J Phys Chem A 2019;123:7007–15. https://doi.org/10.1021/acs.jpca.9b03930.

[14] Rai Y, Neville A, Morina A. Transient processes of MoS_2 tribofilm formation under boundary lubrication. Lubr Sci 2016;28:449–71. https://doi.org/10.1002/ls.1342.

[15] Komaba M, Kondo S, Suzuki A, Kurihara K, Mori S. The effect of temperature on lubrication property with MoDTC-containning lubricant : temperature dependence of friction coefficient and tribofilm structure. Tribol Online 2018;13:275–81. https://doi.org/10.2474/trol.13.275.

[16] Coffey TA, Forster GD, Hogarth G. Molybdenum(VI) imidodisulfur complexes formed via double sulfur–carbon bond cleavage of dithiocarbamates. J Chem Soc Dalton Trans 1996:183–93. https://doi.org/10.1039/DT9960000183.

[17] Farmer HH, Rowan EV. Lubricating compositions containing sulfurized oxymolybdenum dithiocarbamates. US3509051A, 1970.

[18] Guibert M, Nauleau B, Kapsa, P, Rigaud E. Design and manufacturing of a reciprocating linear tribometre. Tribol. Couplages Multi-Phys. Lille, Lille: 2006.

[19] Wagner CD, Davis LE, Zeller MV, Taylor JA, Raymond RH, Gale LH. Empirical atomic sensitivity factors for quantitative analysis by electron spectroscopy for chemical analysis. Surf Interface Anal 1981;3:211–25. https://doi.org/10.1002/sia.740030506.

[20] Deshpande P, Minfray C, Dassenoy F, Thiebaut B, Le Mogne T, Vacher B, et al. Tribological behaviour of TiO2 Atmospheric Plasma Spray (APS) coating under mixed and boundary lubrication conditions in presence of oil containing MoDTC. Tribol Int 2018;118:273–86. https://doi.org/10.1016/j.triboint.2017.10.003.
[21] Spevack PA, McIntyre NS. A Raman and XPS investigation of supported molybdenum oxide thin films. 2. Reactions with hydrogen sulfide. J Phys Chem 1993;97:11031–6. https://doi.org/10.1021/j100144a021.
[22] Benoist L, Gonbeau D, Pfister-Guillouzo G, Schmidt E, Meunier G, Levasseur A. X-ray photoelectron spectroscopy characterization of amorphous molybdenum oxysulfide thin films. Thin Solid Films 1995;258:110–4. https://doi.org/10.1016/0040-6090(94)06383-4.
[23] Fu W, Yang S, Yang H, Guo B, Huang Z. 2D amorphous MoS3 nanosheets with porous network structures for scavenging toxic metal ions from synthetic acid mine drainage. J Mater Chem A 2019;7:18799–806. https://doi.org/10.1039/C9TA05861C.
[24] McIntyre NS, Spevack PA, Beamson G, Briggs D. Effects of argon ion bombardment on basal plane and polycrystalline MoS2. Surf Sci 1990;237:L390–7. https://doi.org/10.1016/0039-6028(90)90508-6.
[25] Khaemba DN, Neville A, Morina A. A methodology for Raman characterisation of MoDTC tribofilms and its application in investigating the influence of surface chemistry on friction performance of MoDTC lubricants. Tribol Lett 2015;59:1–17. https://doi.org/10.1007/s11249-015-0566-6.
[26] Oumahi C, De Barros-Bouchet MI, Le Mogne T, Charrin C, Loridant S, Geantet C, et al. MoS2 formation induced by amorphous MoS3 species under lubricated friction. RSC Adv 2018;8:25867–72. https://doi.org/10.1039/C8RA03317J.
[27] Morina A, Neville A, Priest M, Green JH. ZDDP and MoDTC interactions and their effect on tribological performance - Tribofilm characteristics and its evolution. Tribol Lett 2006;24:243–56. https://doi.org/10.1007/s11249-006-9123-7.
[28] De Faria DLA, Venâncio Silva S, De Oliveira MT. Raman microspectroscopy of some iron oxides and oxyhydroxides. J Raman Spectrosc 1997;28:873–8.
[29] Dieterle M, Weinberg G, Mestl G. Raman spectroscopy of molybdenum oxides. Phys Chem Chem Phys 2002;4:812–21. https://doi.org/10.1039/B107012F.
[30] Espejo C, Thiébaut B, Jarnias F, Wang C, Neville A, Morina A. MoDTC tribochemistry in steel/steel and steel/diamond-like-carbon systems lubricated with model lubricants and fully formulated engine oils. J Tribol 2019;141. https://doi.org/10.1115/1.4041017.
[31] Dieterle M, Mestl G. Raman spectroscopy of molybdenum oxides. Phys Chem Chem Phys 2002;4:822–6. https://doi.org/10.1039/B107046K.
[32] Sahoo S, Gaur APS, Ahmadi M, Guinel MJ-F, Katiyar RS. Temperature-dependent Raman studies and thermal conductivity of few-layer MoS2. J Phys Chem C 2013;117:9042–7. https://doi.org/10.1021/jp402509w.
[33] Seo B, Jung GY, Lee SJ, Baek DS, Sa YJ, Ban HW, et al. Monomeric MoS42−-Derived Polymeric Chains with Active Molecular Units for Efficient Hydrogen Evolution Reaction. ACS Catal 2019. https://doi.org/10.1021/acscatal.9b02700.
[34] Sakurai T, Okabe H, Isoyama H. The Synthesis of Di-μ-thio-dithio-bis (dialkyldithiocarbamates) Dimolybdenum (V) and Their Effects on Boundary Lubrication. Bull Jpn Pet Inst 1971;13:243–9. https://doi.org/10.1627/jpi1959.13.243.